gout, urate, and crystal deposition disease

MDPI

Article

Assessing Changes in Vascular Inflammation and Urate Deposition in the Vasculature of Gout Patients After Administration of Pegloticase Using Positron Emission Tomography and Dual-Energy Computed Tomography—A Pilot Study

Ira Khanna [1,*], Venkatesh Mani [2], Renata Pyzik [2], Audrey Kaufman [2], Weiwei Chi [1], Emilia Bagiella [3], Philip Robson [2] and Yousaf Ali [1]

[1] Division of Rheumatology, Department of Internal Medicine, Icahn School of Medicine, Mount Sinai, New York, NY 10029, USA
[2] Biomedical Engineering and Imaging Institute and Department of Radiology, Icahn School of Medicine, Mount Sinai, New York, NY 10029, USA
[3] Department of Population Health Science and Policy, Icahn School of Medicine, Mount Sinai, New York, NY 10029, USA
* Correspondence: ira.khanna@mountsinai.org

Abstract: We assessed changes in vascular inflammation and monosodium urate (MSU)-coded deposits after administration of Pegloticase in the vasculature of tophaceous gout patients using ^{18}F-fluorodeoxyglucose (^{18}F-FDG) Positron emission tomography/computed tomography (PET/CT) and dual-energy CT (DECT). Ten patients with tophaceous gout, intolerant or refractory to urate-lowering therapy (ULT), were treated with Pegloticase every two weeks for six months. ^{18}F-FDG PET/CT and DECT were performed at baseline and after Pegloticase therapy to detect vessel wall inflammation (Standard uptake value, SUVmean, and SUVmax) and vascular MSU-coded deposition (MSU volume). Data were summarized using means and standard deviations. Baseline and follow-up values were compared for each variable using mixed-effect models. Significant decreases in SUVmean (p = 0.0003) and SUVmax (p = 0.009) were found with a trend towards a decrease in vessel wall MSU volume after treatment. There was a significant decrease in serum urate, correlating with reduction in SUVmean (R^2 = 0.65), with a trend towards a decrease in CRP and blood pressure in all patients. Despite the small sample size, we were able to demonstrate a decrease in vessel wall inflammation and a trend towards a decrease in MSU volume by intensively lowering serum urate. These findings suggest that MSU-coded deposits and hyperuricemia may play a role in vascular wall inflammation. It remains to be seen whether this correlates with a decrease in adverse cardiovascular outcomes.

Keywords: gout; cardiovascular inflammation

check for updates

Citation: Khanna, I.; Mani, V.; Pyzik, R.; Kaufman, A.; Chi, W.; Bagiella, E.; Robson, P.; Ali, Y. Assessing Changes in Vascular Inflammation and Urate Deposition in the Vasculature of Gout Patients After Administration of Pegloticase Using Positron Emission Tomography and Dual-Energy Computed Tomography—A Pilot Study. *Gout Urate Cryst. Depos. Dis.* **2024**, 2, 339–353. https://doi.org/10.3390/gucdd2040024

Received: 2 July 2024
Revised: 17 October 2024
Accepted: 29 October 2024
Published: 6 November 2024

Copyright: © 2024 by the authors. Published by MDPI on behalf of the Gout, Hyperuricemia and Crystal Associated Disease Network. Licensee MDPI, Basel, Switzerland. This article is an open access article distributed under the terms and conditions of the Creative Commons Attribution (CC BY) license (https://creativecommons.org/licenses/by/4.0/).

1. Introduction

Gout is the most common inflammatory arthritis, caused by hyperuricemia and subsequent deposition of aggregated monosodium urate (MSU) crystals in both articular and extra-articular regions including soft tissues and kidneys (uric acid stones) [1,2]. There is a strong association between asymptomatic hyperuricemia, gout, and risk of cardiovascular disease [3–6]. Several retrospective studies have found asymptomatic hyperuricemia and gout to be independent risk factors for myocardial infarction, heart failure, and stroke [7–9]. Asymptomatic hyperuricemia and the presence of tophi have also been associated with an increased risk of mortality in people with gout [10]. Data from the National Health and Nutrition Examination Survey (NHANES) and the Rotterdam studies have in fact demonstrated an association between asymptomatic hyperuricemia and cardiovascular mortality [11,12]. Asymptomatic hyperuricemia has also been seen to be associated with increased levels of inflammatory markers such as C-reactive protein (CRP), tumor necrosis

factor, and interleukin-1, which are risk factors for adverse cardiovascular outcomes [13,14]. Another strong marker has been the discovery of MSU deposits on histopathology and imaging of vessel walls within atherosclerotic plaques and sites of aneurysms [15–18]. The NOR Gout study found associations between MSU-coded deposition in carotid arteries using ultrasound and dual energy computed tomography (DECT), serum calprotectin levels and carotid intima-media thickness, and presence of plaques. These results suggest that crystal deposition may contribute to subclinical inflammation with possibly subsequent vascular disease [19].

In a recent prospective study, the volume of MSU crystal deposition in patients' knees and feet, as measured by DECT, was found to be a biomarker for the risk of developing new-onset cardiovascular disease and for all-cause mortality [20]. Tophus volume has also been shown to correlate with cardiovascular risk, as measured by the Framingham risk score, and metabolic syndrome-related comorbidities. People with gout with positive DECT results have significantly higher systolic and diastolic blood pressures, fasting glucose, and higher prevalence of chronic kidney disease compared with those with negative DECT results [21]. DECT has also been shown to be able to detect MSU-coded deposition in the vasculature of patients with gout [22–24]. In another study, this increase in the frequency of cardiovascular MSU-coded deposits in people with gout was associated with elevated coronary calcium score [23]. Large meta-analyses have demonstrated a dose-dependent association between asymptomatic hyperuricemia and hypertension, with every 1 mg/dL increase in serum urate increasing the risk of hypertension by 13–15% [25,26].

The effect of urate-lowering therapy (ULT) on cardiovascular risk has also been studied. Allopurinol has been shown to improve endothelial function by reversing the effects of decreased levels of nitric oxide on the endothelium and decreasing flow-mediated vasodilation [27,28]. It is also associated with decreased blood pressure and a decreased risk of incident myocardial infarctions, strokes, peripheral arterial disease, and atrial fibrillation in the Medicare population [29–33]. A post hoc analysis of two Pegloticase randomized controlled trials demonstrated that patients who maintained a persistently lower serum urate level had significant reductions in both systolic and diastolic blood pressure that were independent of changes in renal function [34]. Despite the strong cross-sectional evidence linking serum urate (SU) levels and MSU burden to systemic inflammation and cardiovascular risk, a specific association with vascular inflammation has not been shown.

Vascular ^{18}F-fluorodeoxyglucose (^{18}F-FDG) Positron Emission Tomography (PET/CT) has been extensively validated as a measure of arterial vessel wall inflammation in atherosclerosis, with histologic corroboration in human and animal disease models. Subsequently, vascular ^{18}F-FDG PET/CT is often used as a non-invasive surrogate marker of anti-atheroma drug efficacy [35–40].

We postulated that elevated SU and MSU-coded deposits in the vasculature may cause systemic and local vascular inflammation, which results in the progression of atherosclerosis and facilitates early onset of cardiovascular events. Our aim was to show that a decline in SU levels and MSU-coded deposition mediated by intensive ULT is correlated with a decrease in vascular inflammation.

2. Materials and Methods

This study was approved by the Institutional Review Board (IRB). Ten patients with tophaceous gout who were either intolerant or refractory to oral ULT were recruited after obtaining signed consent, using an official medical interpreter when needed. We excluded patients who were diabetics on insulin, had claustrophobia that would limit the DECT and PET scan, had G6PD deficiency, and those with NYHA Class IV heart failure. ULT comprised infusions of Pegloticase, a pegylated recombinant form of uricase, an enzyme that converts uric acid to inactive, water-soluble metabolite allantoin, hence rapidly decreasing serum uric acid levels. Pegloticase is FDA-approved and available in the United States for chronic gout resistant to standard urate lowering therapy. All patients were prescribed Colchicine to prevent flares with rapid urate lowering. All patients were pre-

treated with low-dose immunomodulators (Azathioprine or Methotrexate) to prevent the formation of anti-drug antibodies (ADAs), starting four weeks prior to Pegloticase infusions. The four week duration of exposure to immunomodulators prior to Pegloticase use was based on prior immunomodulator studies related to Pegloticase efficacy, including the MIRROR trial [41,42]. The decision to use Azathioprine versus Methotrexate was decided based on renal function and medication tolerability. Doses used for immunomodulators were based on prior studies on immunomodulator use with Pegloticase [43]. The patients were then treated with Pegloticase infusions 8mg IV every two weeks for six months as per FDA protocol [44].

^{18}F-FDG PET/CT and DECT imaging studies were performed at baseline and after six months of Pegloticase treatment to detect vascular inflammation and vascular MSU deposition, respectively. Briefly, for ^{18}F-FDG PET/CT, patients were required to have fasted for 4–6 h and have blood glucose <170 mg/dL prior to injection of a 10-mCi dose of ^{18}F-FDG. Following 90 min of tracer circulation, PET/CT imaging (Biograph Vision, Siemens Healthineers GmBH, Erlangen, Germany) was performed from head to knees in 10 min. Image resolution was 3.3 mm. In a separate scan, DECT imaging was performed using a Dual Source-Dual Detector Siemens Somatom Force CT scanner (Siemens Healthineers GmBH, Erlangen, Germany). Image resolution was 0.2 mm. Imaging spanned from head to knees with energy levels of 80 kV and 150 kV (tin filter), beam currents of 81 mA and 101 mA, collimation width of 0.6 mm, total collimation width of 57.6 mm, slice thickness 0.6 mm, and pitch of 0.7. A multidensity phantom constructed from MSU crystals suspended in resin with samples ranging from 0–600 mg/cm^3 uric acid was placed on the subject's chest during image acquisition for subsequent visual calibration of image analysis. The average radiation dose per timepoint was as follows (median, interquartile range): effective dose 7.0, 6.9–7.0 mSv for ^{18}F-FDG PET, DLP 577.3, 454.6–883.1 mGy.cm for CT component of PET/CT, and DLP 335.8, 310.7–349.0 mGy.cm for DECT.

Image analysis of PET/CT data was performed as previously described using OsiriX MD (Pixmeo, Geneva, Switzerland) [45]. CT images extending from the level of the carotid artery bifurcation in the neck through the mid-lower extremities were fused with ^{18}F-FDG PET images of the same regions and analyzed in the axial plane. The following target arteries were analyzed: bilateral common carotids, ascending thoracic aorta, descending thoracic aorta, abdominal aorta, bilateral common iliacs, and bilateral femorals. Regions of Interest (ROIs) were manually drawn along the outer boundary of each vessel in the axial plane on the fused images, avoiding PET signal spillover from adjacent structures. The mean and maximum Standardized Uptake Values (SUVs)—a dimensionless parameter indicative of tracer uptake—in each slice (SL) were recorded: SUVmeanSL and SUVmaxSL. In each vessel, several ROIs were drawn on consecutive axial slices as follows: (1) common carotids—just proximal to the bifurcation and extending caudally for a maximum attempted length of 7.5 cm, (2) ascending aorta—just caudal to where the aorta begins to elongate into the arch and extending toward the aortic root to the level where the right atrium is visible, (3) descending thoracic aorta—just caudal to where the aorta elongates from the arch and extends toward the abdomen through the level of the lung fields, (4) abdominal aorta—continuing through to its bifurcation, (5) bilateral common/external iliacs up to the inguinal ligaments, and (6) bilateral femoral arteries from the level where the vessel enters the axial plane for 10 cm caudally. Values for each vessel segment were subsequently reported as SUVmean[vessel] and SUVmax[vessel] by averaging over all slice values in a segment, and finally, values for each patient were reported as SUVmean and SUVmax by averaging over all slices in all vessels. In addition, a Target-to-Background ratio (TBR) was calculated for each slice by normalizing each arterial SUV measure to the background uptake defined as the average SUVmean in the blood pool of nearby veins, i.e., internal jugular veins, superior vena cava, and inferior vena cava. The background was the average SUVmean over 10 slices of ROIs $\geq$25 mm^2 drawn in the relevant vein. Anatomical landmarks were used to provide consistency in vessel segments analyzed from baseline to follow-up.

DECT analysis used the DECT module in the Gout application of the syngo. via an image analysis platform (Siemens Healthineers GmBH, Erlangen, Germany) as previously described [46]. Using dual energies and a material decomposition algorithm, the program highlights urate as bright green. The phantom was used to visually calibrate determine a threshold for detecting MSU. The analyst manually adjusted the minimum Hounsfield unit threshold for material decomposition by selecting either the level at which the signal of the 300 mg/cm^3 (30% *w*/*w*) urate phantom faded from view or that eliminated clearly calcified bony structures from the urate measurement. In a previous phantom study, a threshold of 15% was used for detecting MSU [24]. The volume of each MSU-coded deposit was measured in each slice in the target vessel, summed to give MSU volume in each targeted vessel (MSUvolume[vessel]), and further summed to give total MSU volume for each patient (MSUvolume). The target arteries were identical to the PET portion of the study apart from the extent of the femoral arteries analyzed. For DECT, analysis included the full extent of bilateral common femoral arteries from their origin at the inguinal ligament and branching to the superficial femoral artery up until the popliteal region. DECT and PET analysis were performed in separate sessions.

Blood pressure, serum urate, CRP, Triglycerides (TG), Low-density lipoproteins (LDL), and Hemoglobin A1C at first and last visits were also collected.

Data were summarized using means and standard deviations. Baseline and follow-up values were compared for ^{18}F-FDG uptake variables and MSU volume on a patient level using paired *t*-tests. Vessel segment analyses were conducted using mixed-effect models using subjects and vessel as nested random effects. Paired *t*-tests were used for the comparison of laboratory values and blood pressure. Correlations between patient-level changes in vascular measures and changes in hs-CRP and serum urate pre- and post-Pegloticase treatment were estimated using Pearson's correlation coefficient.

3. Results

Ten patients with tophaceous gout were recruited, out of which six completed more than 10 infusions; the remaining four patients had early terminations due to allergic reactions, becoming non-responders to Pegloticase, which signifies development of anti-drug antibodies, or intravenous line issues (Table 1).

3.1. ^{18}F-FDG-PET and DECT Analysis

Both ^{18}F-FDG uptake and MSU volume were reduced after Pegloticase treatment. On a patient level, reductions were not statistically significant. However, in the mixed effects model analysis of ^{18}F-FDG uptake measures and MSU volume from each vessel segment, a statistically significant reduction in ^{18}F-FDG uptake was observed (SUVmean, $p = 0.0003$ and SUVmax, $p = 0.009$) along with a trend towards a decrease in MSU-coded deposition (MSU volume, $p = 0.75$) (Figure 1, Table 2). In terms of individual vessels, there was a significant decrease in vessel wall inflammation measured by SUVmean for the right carotid artery ($p = 0.0239$) and by SUVmax for the right and left carotid arteries ($p = 0.012$ and $p = 0.0433$, respectively). Average SUV and MSU volumes in individual vessel segments are summarized in Table 3.

3.2. Biomarker Analysis

A statistically significant decrease in SU post-Pegloticase therapy ($p = 0.006$) was observed by a paired *t*-test, with trends towards decreases in CRP and blood pressure in all patients. In a sub-group analysis of patients who completed at least 10 infusions, serum urate remained the only statistically significant change ($p = 0.027$). There was a non-significant increase in serum TG levels post-Pegloticase infusions when all enrolled patients were evaluated, but there was a slight decrease in TG levels in the sub-group analysis of patients who completed greater than 10 infusions (Figure 2). The patients' body weights did not significantly change with treatment.

Table 1. Demographics, adverse events, and eventual early terminations. Six patients completed ≥10 infusions. Four patients terminated early, one due to infusion reaction, two due to losing response for urate lowering which indicates formation of anti-Pegloticase antibodies, and one due to IV line issues.

Patient	Age	Sex	Race	Number of Infusions	Pre-Treatment	Adverse Events Outside of Gout Flares	SU (mg/dL)		CRP (mg/L)		BP (mmHg)		SUVmean		SUVmax		TBRmean		TBRmax		MSU vol/mm^3	
							Pre	Post	Pre	Post	Pre	Post	Pre	Post	Pre	Post	Pre	Post	Pre	Post	Pre	Post
1	53	M	Other- Non-Hispanic	12	Methotrexate 15 mg weekly	-	5.4	<2	1.3	0.5	110/71	110/66	1.81	1.72	2.38	2.30	1.39	1.45	1.83	1.92	5.72	5.94
2	73	M	White	10	Azathioprine 50 mg qday	No adverse effects, stopped due to patient preference	5.3	<1 at 10th, 7.9 on day of last imaging	10.4	1.5	111/65	107/62	1.55	1.64	2.28	2.35	1.15	1.15	1.71	1.65	14.43	32.03
3	77	M	White	12	Azathioprine 50 mg qday	-	9.3	<2	0.4	1.8	136/82	120/66	1.66	1.59	2.21	2.10	1.23	1.36	1.63	1.79	-	-
4	42	M	Asian	2	Methotrexate 15 mg weekly	Early termination due to infusion reaction- mild-rash, pruritis, no hospitalization required	12.2	11.3	46.3	7.4	139/95	140/94	1.64	1.48	2.12	1.91	1.28	1.35	1.66	1.73	2.51	4.25
5	66	M	Hispanic	1	Methotrexate 15 mg weekly	Early termination due to poor IV access	8.7	<2	0.3	0.7	122/79	136/84	1.38	1.45	1.80	1.93	1.35	1.30	1.76	1.73	9.77	1.40
6	50	M	White	12	Azathioprine 100 mg daily	-	11.7	2.1	8	6.8	119/67	108/63	1.91	1.92	2.45	2.47	1.22	1.18	1.56	1.52	1.28	0.0
7	61	M	Asian	2	Methotrexate 15 mg weekly	Early termination, non- responder							2.17	2.19	2.87	2.91	1.36	1.31	1.80	1.73	-	-
8	31	M	Asian	5	Methotrexate 15 mg-> 10 mg-> 12.5 mg weekly	Early termination, became non-responder in terms of uric acid, but tophi were smaller	11.9	10.4	66.5	11.5	131/78	131/83	1.68	1.52	2.17	2.00	1.37	1.32	1.78	1.73	15.45	0.0
9	64	M	Asian	12	Azathioprine 50 mg qday-> Methotrexate 10 mg weekly	Developed drug induced liver injury with Azathioprine, switched to Methotrexate	8.6	<2	80.9	1.2	118/74	109/78	1.58	1.44	2.12	1.95	1.26	1.26	1.67	1.70	6.36	0.0
10	59	M	Asian	12	Methotrexate 15 mg weekly	-	11.9	<2	3.7	13.7	105/67	107/67	1.51	1.45	2.04	2.03	1.36	1.17	1.82	1.63	0.0	0.0

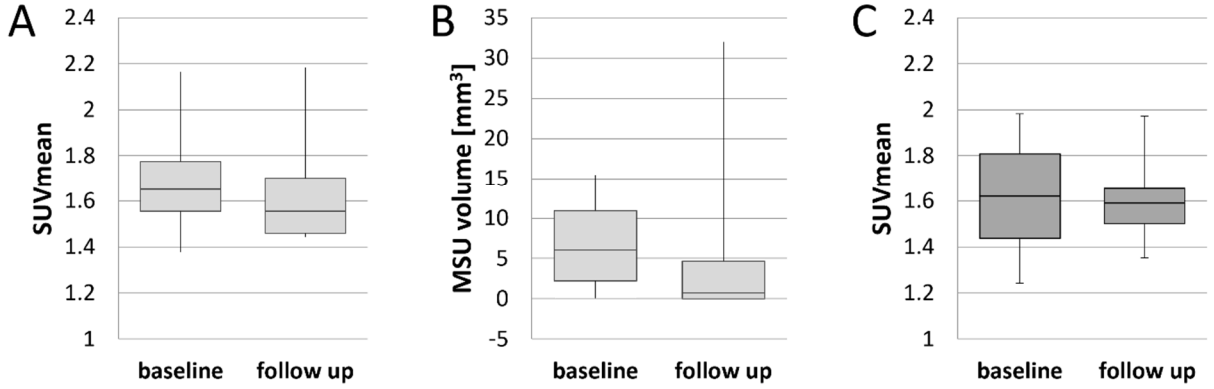

Figure 1. (**A**) ^{18}F-FDG uptake and (**B**) MSU volume on a patient level before and after treatment with Pegloticase. Reductions in SUVmean (averaged over all vessels) and MSU volume (total volume for each patient) after treatment with Pegloticase were not statistically significant, $p = 0.14$ and $p = 0.68$, respectively. (**C**) ^{18}F-FDG uptake in vessel segments with MSU deposits before and after treatment were not statistically significant, $p = 0.86$. Plots show median and inter-quartile range.

Table 2. Results of patient-level and vessel-level analysis with paired *t*-tests and mixed-effects-model analysis, respectively. Positive difference (baseline–follow-up) represents decrease in value at follow-up. At the vessel level, we observed a statistically significant decrease in SUVmean ($p = 0.0003$) and SUVmax ($p = 0.0090$) at follow-up and a trend towards a decrease in TBRmean, TBRmax, and MSU volume at follow-up (not statistically significant).

		SUVmean	SUVmax	TBRmean	TBRmax	MSU vol/mm^3
Patient level	**Reduction from baseline to follow-up**	0.047	0.048	0.013	0.0088	1.49
	***p*-value**	0.14	0.22	0.63	0.78	0.68
Vessel level	**Reduction from baseline to follow-up**	0.050	0.048	0.013	0.0066	0.16
	***p*-value**	**0.0003**	**0.0090**	0.48	0.77	0.75

Table 3. Vessel segment PET and DECT measurements. Quantitative PET values SUVmean and SUVmax [mean (SD)] for individual vessel segments across the cohort of 10 patients pre- and post-treatment. MSU volume [total volume (number of discrete MSU foci)] for individual vessel segments. RCC: right common carotid, LCC: left common carotid, ATA: ascending thoracic aorta, DTA: descending thoracic aorta, DAA: descending abdominal aorta, RIL: right iliac, LIL: left iliac, RFA: right femoral artery, LFA: left femoral artery.

Vessel Segment	**SUVmean**		**SUVmax**		**MSU Volume (mm^3)**	
	Pre	**Post**	**Pre**	**Post**	**Pre**	**Post**
RCC	1.80 (0.26)	1.64 (0.29)	2.14 (0.33)	1.99 (0.28)	0	0
LCC	1.78 (0.29)	1.64 (0.25)	2.10 (0.28)	2.01 (0.26)	3.76 (1)	0
ATA	2.03 (0.37)	1.89 (0.30)	2.77 (0.37)	2.74 (0.44)	0	0
DTA	1.95 (0.34)	1.83 (0.25)	2.54 (0.32)	2.51 (0.33)	1.25 (1)	9.33 (2)
DAA	1.92 (0.32)	1.8 (0.32)	2.47 (0.34)	2.44 (0.47)	25.0 (9)	0.86 (1)
RIL	1.77 (0.34)	1.66 (0.32)	2.20 (0.33)	2.20 (0.41)	2.13 (1)	23.1 (2)
LIL	1.65 (0.31)	1.57 (0.28)	2.07 (0.36)	2.08 (0.37)	0	4.11 (1)
RFA	1.45 (0.39)	1.32 (0.25)	1.92 (0.41)	1.87 (0.35)	5.51 (1)	4.64 (1)
LFA	1.50 (0.36)	1.41 (0.28)	1.97 (0.36)	1.91 (0.37)	17.8 (4)	1.55 (1)

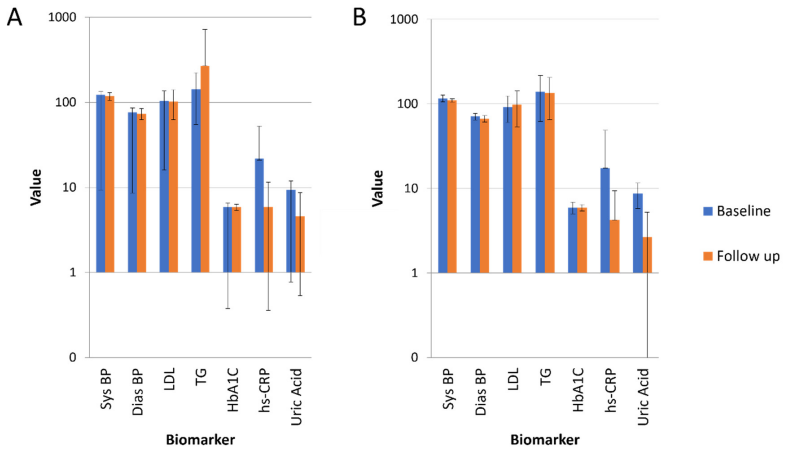

Figure 2. (**A**) Analysis of blood biomarkers for all patients before (baseline) and after Pegloticase infusions (follow-up). By paired *t*-tests, uric acid is the only marker that drops significantly after treatment ($p = 0.006$). (**B**) In a sub-analysis of patients who completed at least 10 infusions, uric acid remains the only statistically significant change ($p = 0.027$). Biomarkers [units]: Sys BP = systolic blood pressure [mmHg]. Dias BP = diastolic blood pressure [mmHg], LDL = low density lipoprotein [mg/dL], TG = triglycerides [mg/dL], HbA1c = hemoglobin A1c [%], hs-CRP = high-sensitivity C-reactive protein [mg/L], uric acid [mg/dL].

3.3. Correlation Analysis

Overall, there were weak correlations between the changes in vascular measures and the changes in blood biomarkers of inflammation (hs-CRP) and serum urate, which improved slightly in sub-group analysis of those patients who completed at least 10 infusions (Table 4). The strongest correlations were between change in serum urate and changes in SUVmean ($R^2 = 0.27$) and MSU volume ($R^2 = 0.88$) when limited to patients who completed at least 10 infusions. Finally, there was a modest correlation between change in MSU volume and change in SUVmean at the patient level with all patients ($R^2 = 0.24$) and in those completing >10 infusion ($R^2 = 0.54$).

Table 4. Sign of correlation and R^2 values from Pearson correlation of patient-level vascular parameters (^{18}F-FDG uptake and MSU volume) against blood marker values CRP and uric acid. Correlations were repeated for all patients and in those patients who completed at least 10 infusions.

		SUVmean	SUVmax	TBRmean	TBRmax	MSU Volume
CRP	**All patients**	+, 0.003	−, <0.001	+, 0.036	+, 0.036	−, 0.046
	≥10 infusions	+, 0.20	+, 0.30	−, 0.37	−, 0.14	−, 0.018
Uric acid	**All patients**	+, 0.16	+, 0.17	−, 0.07	−, 0.11	+, 0.15
	≥10 infusions	+, 0.27	+, 0.17	+, 0.07	−, 0.005	+, 0.88
SUVmean	**All patients**	-	-	-	-	+, 0.24
	≥10 infusions	-	-	-	-	+, 0.54

3.4. Segments with MSU Deposits

In secondary ad hoc analyses, we explored changes in ^{18}F-FDG signal in specific vessel segments associated with MSU-coded deposits identified on DECT. A total of 14 vessel segments in 7 patients showed MSU-coded deposits. There was no difference in SUVmean before and after treatment in vessels with MSU-coded deposits ($p = 0.86$) based on paired *t*-test analysis (Table 5 and Figure 1). When considering only vessel segments with MSU-coded deposits, correlation analysis showed there was a weak correlation between serum urate and total MSU volume in those who completed at least ten treatment visits ($R^2 = 0.16$), but not overall. There was poor correlation between hs-CRP and MSU volume ($R^2 = 0.004$).

There was a modest correlation between hs-CRP and ^{18}F-FDG uptake (R^2 = 0.27, SUVmean) in those who completed at least ten treatment visits, but not when including patients with early terminations. There was a modest correlation between ^{18}F-FDG uptake and uric acid (R^2 = 0.65, SUVmean), supporting the hypothesis that the effect of treatment, reflected in serum urate, may also have an effect on vascular inflammation (Table 6 and Figure 3).

Table 5. Results of vessel-level analysis in vessel segments with MSU deposits with paired *t*-tests.

	SUVmean	SUVmax	TBRmean	TBRmax	MSU vol/mm^3
Reduction from baseline to follow-up	0.0073	0.027	0.071	0.10	0.85
***p*-value**	0.86	0.6	0.1	0.08	0.7

Table 6. Correlations between imaging measurements (^{18}F-FDG uptake and MSU volume) and blood biomarkers (CRP and uric acid) in vessel segments with MSU deposits. Sign of correlation and R^2 values from Pearson correlation. Correlations were repeated for all patients with MSU deposits and in those patients who also completed at least 10 infusions.

		SUVmean	SUVmax	TBRmean	TBRmax	MSU Volume
CRP	**All patients**	+, 0.052	+, <0.0001	+, <0.0001	−, 0.030	−, 0.02
	≥10 infusions	+, 0.27	+, 0.21	−, 0.0042	−, 0.028	−, 0.004
Uric acid	**All patients**	+, 0.51	+, 0.28	−, 0.031	−, 0.18	+, 0.083
	≥10 infusions	+, 0.65	+, 0.43	−, 0.021	−, 0.19	+, 0.16
SUVmean	**All patients**	-	-	-	-	+, 0.059
	≥10 infusions	-	-	-	-	+, 0.035

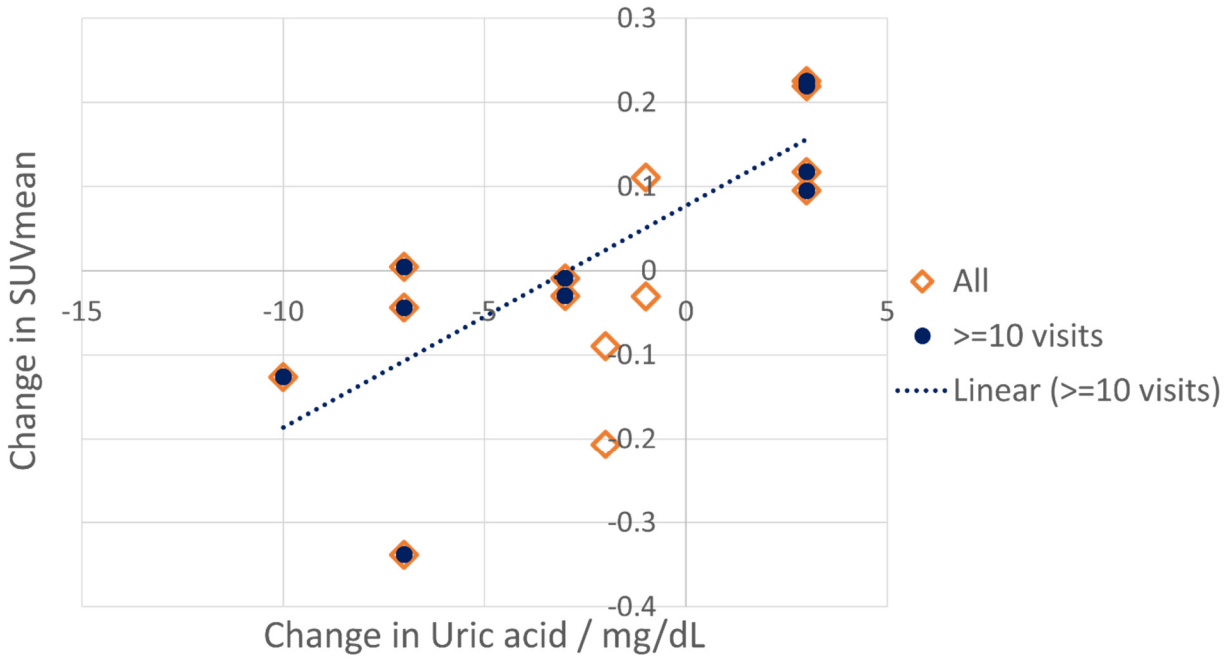

Figure 3. Correlation between changes from baseline to after treatment in ^{18}F-FDG uptake (SUVmean) in vessel segments showing MSU-coded deposits and in uric acid. Moderate correlations were found for all patients with vessel segments showing MSU deposits (R^2 = 0.51) and for patients completing at least 10 visits (R^2 = 0.65).

Representative ^{18}F-FDG PET/CT and DECT images before and after Pegloticase treatment are shown in Figure 4. One patient demonstrated complete resolution of an MSU-coded deposit located in their abdominal aorta following Pegloticase treatment.

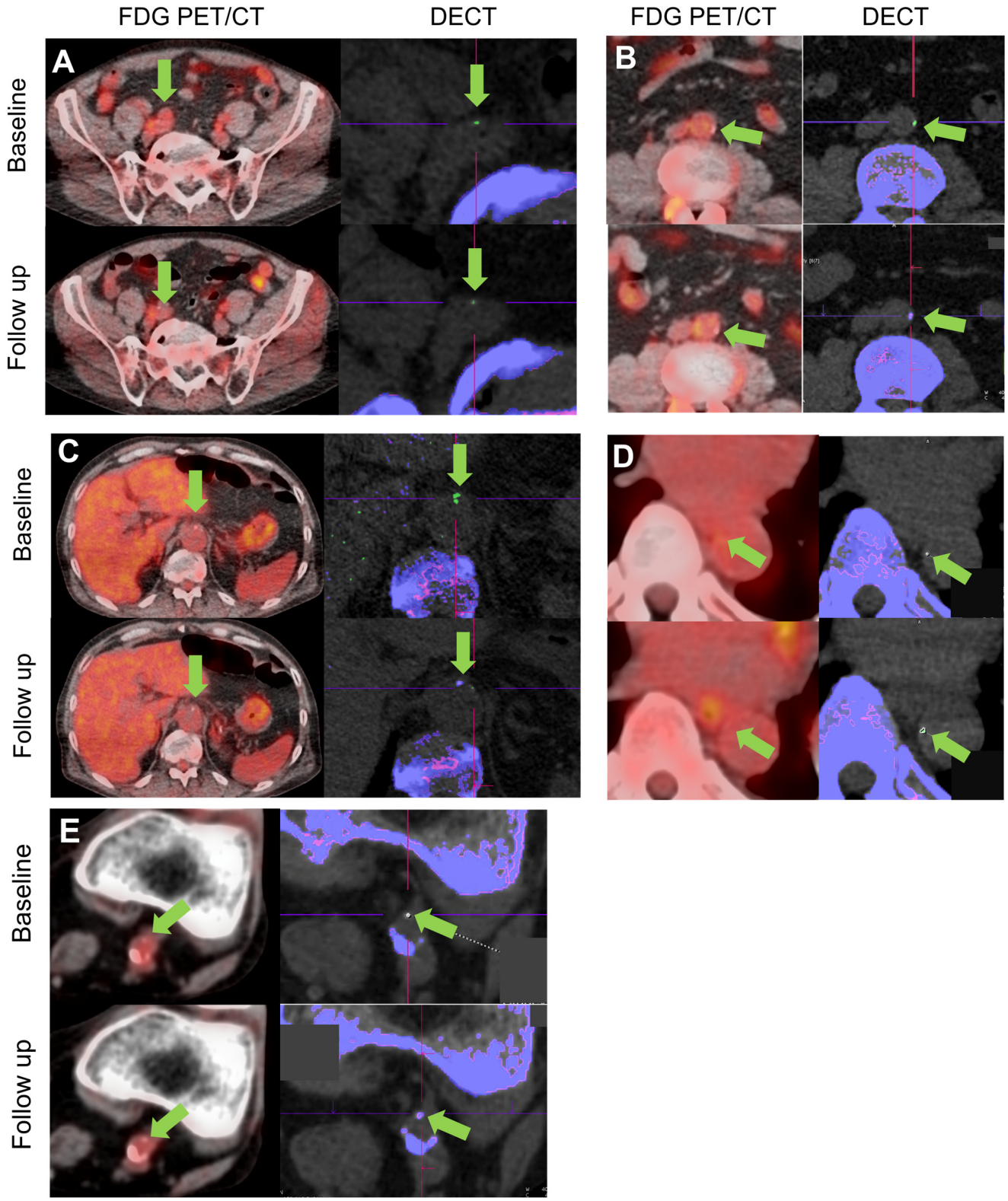

Figure 4. Representative PET/CT (left) and DECT images (right) from axial locations in five vessel levels in four patients. (**A**) ^{18}F-FDG uptake (orange overlay) shows inflammation in the right iliac artery (green arrow). On DECT, MSU-coded deposits (green) are shown in the corresponding vessel

walls (green arrow), with bone (calcium) shown in purple. In this location, imaging shows a decrease in ^{18}F-FDG uptake and MSU volume from baseline to follow-up following treatment with Pegloticase. (**B**) ^{18}F-FDG uptake showing inflammation and DECT showing an MSU-coded deposit in the abdominal aorta (green arrows). In this patient, the deposit which was identified as MSU-coded at baseline, which likely had mixed calcium and MSU characteristics, appeared to resolve after treatment. ^{18}F-FDG uptake in a small segment (~2 cm) of vessel centered on the location of the MSU-coded deposit showed a reduction in SUVmean from 1.81 to 1.68 and in SUVmax from 2.60 to 2.55. (**C**) ^{18}F-FDG uptake in the abdominal aorta (green arrow) is reduced at follow-up (SUVmean/SUVmax pre: 1.65/2.17, post: 1.57/2.00) while MSU-coded deposit resolves. (**D**) In the descending thoracic aorta, little change is seen in ^{18}F-FDG signal (SUVmean/SUVmax pre: 1.69/2.24, post: 1.64/2.26) while MSU-coded deposit volume increases from 1.3 mm^3 to 3.4 mm^3. (**E**) In the left femoral artery another MSU deposit resolves after treatment while ^{18}F-FDG signal reduces slightly (SUVmean/SUVmax pre: 1.64/2.30, post: 1.64/2.25).

4. Discussion

There has been growing interest in the risk of cardiovascular disease in patients with gout.

The role of DECT in detecting vascular MSU-coded deposits has provided a non-invasive alternative to the detection of MSU crystals via microscopic examination, which is challenging in soft tissues given that formalin or ethanol fixation can cause crystal dissolution or reduce crystal concentration, leading to false negatives [47]. Held et al. demonstrated a higher risk of major adverse cardiac events in patients with DECT-verified vascular MSU-coded deposits compared to those without. These patients also had increased serum acute phase reactants, uric acid levels, and calcium scores compared to those without cardiovascular MSU-coded deposits [48]. A recent review has highlighted several studies showing association of cardiovascular MSU-coded deposits on DECT in gout patients compared to controls, mostly in the coronaries and the aorta, although no difference was found in popliteal artery DECT MSU-coded deposits [49]. In patients with angina, Ren et al. demonstrated that the presence of cardiovascular MSU-coded deposits on DECT was higher in patients with calcified plaques than those without, which were seen more in patients with gout [50]. A retrospective study focusing on artefacts in DECT by Yokose et al. showed MSU-coded plaques in 85% of gout patients and 84% of controls. Advanced DECT measurements using electron density (Rho) and effective atomic number detected all green spots as artefacts [51]. The VASCURATE study showed that DECT-based vascular MSU-coded plaques in peripheral arteries was comparable in gout patients (24.6%) and controls (23.1%; p = 0.87). Vascular MSU-coded plaques were also strongly associated with coexisting arterial calcifications but not with soft-tissue MSU deposition. These findings suggest that DECT-based MSU-coded plaques in peripheral arteries may not reflect genuine MSU crystal deposition and thus should not be a primary target while treating gout patients [52].

Vascular ^{18}F-FDG PET/CT imaging of the aorta and carotid vessels is a well-established non-invasive measure of vascular inflammation and cardiovascular risk. We observed a statistically significant reduction in vessel wall inflammation (SUV mean and SUV max) following treatment with Pegloticase, indicating the presence of an association between hyperuricemia and vascular inflammation, a known marker of cardiovascular risk. A reduction in vascular inflammation was correlated with a reduction in serum urate levels, supporting the hypothesis that uric acid may also have an effect on vascular inflammation. These data suggest a role for ULT in mitigating cardiovascular risk in gout.

We observed a non-significant trend towards a decrease in vascular MSU-coded deposition (MSU volume) in tophaceous gout patients following treatment with Pegloticase. The duration of treatment may not have been sufficient to observe robust reduction in MSU volume. Overall, we observed no evidence of continued growth while undergoing urate-lowering therapy with Pegloticase; however, increases were observed in some vessel segments. Our DECT results do not provide proof of MSU deposits and, per the VASCU-

RATE study, may be confounded by calcium deposits; however, the findings are interesting in their own light associated with the decreased inflammation and changes in biomarkers. Given the small cohort size, it was not possible to assess the effect of imaging limitations on these observations. The impact of MSU-coded deposit burden independently from serum urate levels remains to be determined.

Our study has various limitations. Our sample size was small, with only ten patients. We were recruiting in the middle of a global pandemic, which resulted in challenges with recruitment and retention. We also had four patients who had early terminations—one due to intravenous line placement issues, one who had a reaction, and two who became non-responders—which could be contributing to bias (Table 1). However, we carried out a subgroup analysis for completers, defined as patients who received more than ten infusions, that showed similar findings (Figures 2 and 3, Tables 3 and 5). We did not have a control population in this small pilot study and cannot rule out changes occurring as a part of natural progression. Future studies should include a control population for a more accurate comparison. We did not perform microscopic confirmation of vascular MSU crystals given the limitations of vascular biopsies in living patients, as opposed to cadaver studies that have been able to confirm microscopic MSU correlating with DECT MSU detection [23,53].

While changes in SUV were statistically significant, those in TBR were not. This may be due to additional variance in background blood pool SUV measurements and a small effect size limiting statistical power in this small study. Additionally, the degree of ^{18}F-FDG uptake and inferred inflammation were subtle, suggesting that larger cohorts may be required to detect statistically significant changes.

We found a low burden of vascular MSU-coded deposits in this cohort, which may have limited the evaluation of MSU deposition. Additionally, the DECT results of two patients were not interpretable due to extensive image artifacts, which further limited data aggregation. Measurement of MSU-coded deposits using DECT was also likely limited by the small size of the deposits found in this cohort, as previously discussed by Dossing et al., who noted that deposits <2 mm in diameter could not be considered to represent MSU with confidence [54]. Identification of vascular deposits may also be limited by the motion of the vessel wall during the acquisition of the CT image data. In some cases, deposits coded as MSU were subsequently coded as calcium. This may indicate "mixed" MSU and calcium deposits or may be an artifact as noted previously by Dossing et al. and Toprover et al. [54,55]. Furthermore, it may be necessary to optimize DECT parameters for separating MSU from calcium deposits [55]. However, both this approach and our use of adjusting image levels to eliminate the 300 cm^3 phantom or the bony structures from the urate signal may be excluding actual MSU. In future work, physical phantoms with finer gradations of MSU content will be useful to explore mis-coding of calcium as MSU. Ultimately, DECT may perform better when larger quantities of MSU are present. Further studies, including with dedicated phantoms [24], are required to optimize the detection of vascular MSU using DECT.

All of our patients took low-dose Methotrexate or Azathioprine to prevent the formation of neutralizing antibodies with self-reported adherence. We did consider that the decrease in vessel wall inflammation could be from the Methotrexate and Azathioprine, which were initiated four weeks prior to Pegloticase infusions. Although we accept this is a potential confounder, we feel that the drugs had probably not reached their maximal anti-inflammatory effect during the study. The use of these agents are standard of care, FDA-approved, and necessary to ensure Pegloticase was appropriately tolerated [56]. Also important to consider is that these medications were used at lower doses compared to doses used in other studies looking at the effect of Methotrexate on vascular PET [57]. Another confounding factor could be the effect of Colchicine on vascular inflammation. However, all our patients were already on Colchicine prior to study initiation and were continued on their home dose.

Differences in inflammation in individual vessels were evaluated, including the carotids, ascending and descending thoracic aorta, iliac, and femoral arteries, but did

not include the coronaries. In future studies, it would also be interesting to correlate vascular MSU deposition with coronary calcium scores. Studies have shown that silent MSU deposition in joints of patients with asymptomatic hyperuricemia (detected by ultrasound) was associated with more severe coronary calcification, which suggests more severe CAD in relation to crystal deposition [58].

Finally, while this study provides insight into vascular inflammation and cardiovascular disease in patients with gout, given the radiation exposure, it may not be appropriate in routine clinical evaluation.

5. Conclusions

In conclusion, despite the small sample size of our study, we were able to demonstrate a significant decrease in vessel wall inflammation and a trend towards decreased MSU-coded deposition in tophaceous gout patients by aggressively lowering serum urate. These findings demonstrate a specific association between serum urate levels and vascular inflammation, suggesting a role of urate-lowering therapy in mitigating cardiovascular risk. Further studies are warranted to investigate the role of MSU-coded deposits in vascular inflammation, and larger, longitudinal studies are required to assess the impact of ULT on adverse cardiovascular outcome.

Author Contributions: Conceptualization, V.M., Y.A. and I.K.; Methodology, V.M., Y.A., I.K., P.R., R.P., W.C. and A.K.; validation, P.R., R.P. and A.K.; formal analysis, E.B., P.R., A.K., V.M., I.K., W.C. and Y.A.; investigation, I.K., R.P., Y.A., W.C., A.K. and P.R.; resources, R.P., A.K., P.R. and E.B.; data curation, P.R., V.M., Y.A., I.K., R.P., A.K. and W.C.; writing—original draft preparation, I.K.; writing—review and editing, Y.A., V.M., P.R., W.C., A.K. and E.B.; visualization, I.K., Y.A., P.R., A.K., V.M. and W.C.; supervision, V.M. and Y.A.; project administration, R.P.; funding acquisition, Y.A. and V.M. All authors have read and agreed to the published version of the manuscript.

Funding: Horizon Therapeutics, no role in design or analysis of study.

Institutional Review Board Statement: The study was conducted in accordance with the Declaration of Helsinki, and approved by the Institutional Review Board of Mount Sinai School of Medicine , in accordance with Mount Sinai's Federal Wide Assurances (GCO 19-2826, FWA#00005656, FWA#00005651) to the Department of Health and Human Services from 21 September 2021 to 27 September 2023.

Informed Consent Statement: Informed consent was obtained from all subjects involved in the study.

Data Availability Statement: All data supporting the reported results are included in the manuscript. Patient-specific data are unavailable due to privacy restrictions.

Conflicts of Interest: The authors declare no conflicts of interest. The funders had no role in the design of the study; in the collection, analyses, or interpretation of data; in the writing of the manuscript; or in the decision to publish the results.

References

1. Euler, A.; Wullschleger, S.; Sartoretti, T.; Müller, D.; Keller, E.X.; Lavrek, D.; Donati, O. Dual-energy CT kidney stone characterization-can diagnostic accuracy be achieved at low radiation dose? *Eur. Radiol.* **2023**, *3*, 6238–6244. [CrossRef] [PubMed] [PubMed Central]
2. Johnson, J.P.; Dhall, A.; Chawla, A.; Prakashini, K. Renal calculus composition analysis using dual-energy CT: A prospective observational study. *Afr. J. Urol.* **2024**, *30*, 19. [CrossRef]
3. Abbott, R.D.; Brand, F.N.; Kannel, W.B.; Castelli, W.P. Gout and coronary heart disease: The Framingham study. *J. Clin. Epidemiol.* **1988**, *41*, 237–242. [CrossRef] [PubMed]
4. Krishnan, E.; Baker, J.F.; Furst, D.E.; Schumacher, H.R. Gout and the risk of acute myocardial infarction. *Arthritis Rheum.* **2006**, *54*, 2688–2696. [CrossRef] [PubMed]
5. Choi, H.K.; Curhan, G. Independent impact of gout on mortality and risk for coronary heart disease. *Circulation* **2007**, *116*, 894–900. [CrossRef]
6. Kuo, C.F.; Yu, K.H.; See, L.C.; Chou, I.J.; Ko, Y.S.; Chang, H.C.; Luo, S.F. Risk of myocardial infarction among patients with gout: A nationwide population-based study. *Rheumatology* **2013**, *52*, 111–117. [CrossRef]
7. Krishnan, E.; Pandya, B.J.; Lingala, B.; Hariri, A.; Dabbous, O. Hyperuricemia and untreated gout are poor prognostic markers among those with a recent acute myocardial infarction. *Arthritis Res. Ther.* **2012**, *14*, R10. [CrossRef]

8. Casiglia, E.; Tikhonoff, V.; Virdis, A.; Masi, S.; Barbagallo, C.M.; Bombelli, M.; Borghi, C. Serum uric acid and fatal myocardial infarction: Detection of prognostic cut-off values: The URRAH (Uric acid right for heart health) study. *J. Hypertens.* **2020**, *38*, 412–419. [CrossRef]
9. Singh, J.A.; Ramachandaran, R.; Yu, S.; Yang, S.; Xie, F.; Yun, H.; Zhang, J.; Curtis, J.R. Is gout a risk equivalent to diabetes for stroke and myocardial infarction? A retrospective claims database study. *Arthritis Res. Ther.* **2017**, *19*, 228. [CrossRef]
10. Perez-Ruiz, F.; Martínez-Indart, L.; Carmona, L.; Herrero-Beites, A.M.; Pijoan, J.I.; Krishnan, E. Tophaceous gout and high level of hyperuricaemia are both associated with increased risk of mortality in patients with gout. *Ann. Rheum. Dis.* **2014**, *73*, 177–182. [CrossRef]
11. Fang, J.; Alderman, M.H. Serum uric acid and cardiovascular mor- tality the NHANES I epidemiologic follow-up study, 1971–1992. National Health and Nutrition Examination Survey. *JAMA* **2000**, *283*, 2404–2410. [CrossRef] [PubMed]
12. Bos, M.J.; Koudstaal, P.J.; Hofman, A.; Witteman, J.C.; Breteler, M.M. Uric acid is a risk factor for myocardial infarction and stroke: The Rotterdam study. *Stroke* **2006**, *37*, 1503–1507. [CrossRef] [PubMed]
13. Ridker, P.M.; Everett, B.M.; Thuren, T.; MacFadyen, J.G.; Chang, W.H.; Ballantyne, C.; Fonseca, F.; Nicolau, J.; Koenig, W.; Anker, S.D.; et al. Antiinflammatory therapy with canakinumab for atherosclerotic disease. *N. Engl. J. Med.* **2017**, *377*, 1119–1131. [CrossRef]
14. Jalal, D.I.; Jablonski, K.L.; McFann, K.; Chonchol, M.B.; Seals, D.R. Vascular endothelial function is not related to serum uric acid in healthy adults. *Am. J. Hypertens.* **2012**, *25*, 407–413. [CrossRef] [PubMed]
15. Hench, P.S.; Darnall, C.M. A clinic on acute old-fashioned gout; with special reference to its inciting factors. *Med. Clin. N. Am.* **1933**, *16*, 1371–1393.
16. Park, J.J.; Roudier, M.P.; Soman, D.; Mokadam, N.A.; Simkin, P.A. Prevalence of birefringent crystals in cardiac and prostatic tissues, an observational study. *BMJ Open.* **2014**, *4*, e005308. [CrossRef]
17. Patetsios, P.; Song, M.; Shutze, W.P.; Pappas, C.; Rodino, W.; Ramirez, J.A.; Panetta, T.F. Identification of uric acid and xanthine oxidase in atherosclerotic plaque. *Am. J. Cardiol.* **2001**, *88*, 188–191. [CrossRef] [PubMed]
18. Patetsios, P.; Rodino, W.; Wisselink, W.; Bryan, D.; Kirwin, J.D.; Panetta, T.F. Identification of uric acid in aortic aneurysms and atherosclerotic artery. *Ann. N. Y. Acad. Sci.* **1996**, *800*, 243–245. [CrossRef]
19. Hammer, H.B.; Rollefstad, S.; Semb, A.G.; Jensen, G.; Karoliussen, L.F.; Terslev, L.; Haavardsholm, A.E.; Kvien, T.K.; Uhlig, T. Urate crystal deposition is associated with inflammatory markers and carotid artery pathology in patients with intercritical gout: Results from the NOR-Gout study. *RMD Open* **2022**, *8*, e002348. [CrossRef]
20. Marty-Ané, A.; Norberciak, L.; Andrès, M.; Houvenagel, E.; Ducoulombier, V.; Legrand, J.; Budzik, J.-F.; Pascart, T. Crystal deposition measured with dual-energy computed tomography: Association with mortality and cardiovascular risks in gout. *Rheumatology* **2021**, *60*, 4855–4860. [CrossRef] [PubMed]
21. Lee, K.A.; Ryu, S.R.; Park, S.J.; Kim, H.R.; Lee, S.H. Assessment of cardiovascular risk profile based on measurement of tophus volume in patients with gout. *Clin. Rheumatol.* **2018**, *37*, 1351–1358. [CrossRef] [PubMed]
22. Barazani S, Chi W, Pyzik R, Jacobi A, O'Donnell T, Fayad Z; et al. Detection of uric acid crystals in the vasculature of patients with gout using dual-energy computed tomography (abstract). *Arthritis Rheum.* **2018**, *70* (Suppl. S9), 3584.
23. Klauser, A.S.; Halpern, E.J.; Strobl, S.; Gruber, J.; Feuchtner, G.; Bellmann-Weiler, R.; Weiss, G.; Stofferin, H.; Jaschke, W. Dual-energy computed tomography detection of cardiovascular monosodium urate deposits in patients with gout. *JAMA Cardiol.* **2019**, *4*, 1019–1028. [CrossRef]
24. Feuchtner, G.M.; Plank, F.; Beyer, C.; Schwabl, C.; Held, J.; Bellmann-Weiler, R.; Weiss, G.; Gruber, J.; Widmann, G.; Klauser, A.S. Monosodium Urate Crystal Deposition in Coronary Artery Plaque by 128-Slice Dual-Energy Computed Tomography: An Ex Vivo Phantom and In Vivo Study. *J. Comput. Assist. Tomogr.* **2021**, *45*, 856–862. [CrossRef] [PubMed]
25. Grayson, P.C.; Kim, S.Y.; LaValley, M.; Choi, H.K. Hyperuricemia and incident hypertension: A systematic review and meta-analysis. *Arthritis Care Res.* **2011**, *63*, 102–110. [CrossRef]
26. Wang, J.; Qin, T.; Chen, J.; Li, Y.; Wang, L.; Huang, H.; Li, J. Hyperuricemia and risk of incident hypertension: A systematic review and meta-analysis of observational studies. *PLoS ONE* **2014**, *9*, e114259. [CrossRef]
27. Melendez-Ramirez, G.; Perez-Mendez, O.; Lopez-Osorio, C.; Kuri- Alfaro, J.; Espinola-Zavaleta, N. Effect of the treatment with allopu- rinol on the endothelial function in patients with hyperuricemia. *Endocr. Res.* **2012**, *37*, 1–6. [CrossRef]
28. Feig, D.I.; Kang, D.H.; Johnson, R.J. Uric acid and cardiovascular risk. *N. Engl. J. Med.* **2008**, *359*, 1811–1821. [CrossRef]
29. Feig, D.I.; Soletsky, B.; Johnson, R.J. Effect of allopurinol on blood pressure of adolescents with newly diagnosed essential hyperten- sion: A randomized trial. *JAMA* **2008**, *300*, 924–932. [CrossRef]
30. Singh, J.A.; Yu, S. Allopurinol reduces the risk of myocardial infarc- tion (MI) in the elderly: A study of Medicare claims. *Arthritis Res. Ther.* **2016**, *18*, 209. [CrossRef]
31. Singh, J.A.; Yu, S. Allopurinol and the risk of stroke in older adults receiving medicare. *BMC Neurol.* **2016**, *16*, 164. [CrossRef] [PubMed]
32. Singh, J.A.; Cleveland, J. Allopurinol and the risk of incident periph- eral arterial disease in the elderly: A US Medicare claims data study. *Rheumatology* **2018**, *57*, 451–461. [CrossRef] [PubMed]
33. Singh, J.A.; Yu, S. Allopurinol and the risk of atrial fibrillation in the elderly: A study using Medicare data. *Ann. Rheum. Dis.* **2017**, *76*, 72–78. [CrossRef]

34. Johnson, R.J.; Choi, H.K.; Yeo, A.E.; Lipsky, P.E. Pegloticase Treatment Significantly Decreases Blood Pressure in Patients with Chronic Gout. *Hypertension* **2019**, *74*, 95–101. [CrossRef]
35. Fayad, Z.A.; Mani, V.; Woodward, M.; Kallend, D.; Abt, M.; Burgess, T.; Fuster, V.; Ballantyne, C.M.; Stein, E.A.; Tardif, J.-C.; et al. Safety and efficacy of dalcetrapib on atherosclerotic disease using novel non-invasive multimodality imaging (dal-PLAQUE): A randomised clinical trial. *Lancet* **2011**, *378*, 1547–1559. [CrossRef]
36. Græbe, M.; Pedersen, S.; Borgwardt, L.; Højgaard, L.; Sillesen, H.; Kjær, A. Molecular pathology in vulnerable carotid plaques: Correlation with [18]-fluorodeoxyglucose positron emission tomography (FDG-PET). *Eur. J. Vasc. Endovasc. Surg.* **2009**, *37*, 714–721. [CrossRef]
37. Izquierdo-Garcia, D.; Davies, J.R.; Graves, M.J.; Rudd, J.H.; Gillard, J.H.; Weissberg, P.L.; Fryer, T.D.; Warburton, E.A. Comparison of methods for magnetic resonance-guided [18-F]fluorodeoxyglucose positron emission tomography in human carotid arteries: Reproducibility, partial volume correction, and correlation between methods. *Stroke* **2009**, *40*, 86–93. [CrossRef]
38. Rudd, J.H.; Myers, K.S.; Bansilal, S.; Machac, J.; Rafique, A.; Farkouh, M.; Fuster, V.; Fayad, Z.A. ^{18}Fluorodeoxyglucose positron emission tomography imaging of atherosclerotic plaque inflammation is highly reproducible: Implications for atherosclerosis therapy trials. *J. Am. Coll. Cardiol.* **2007**, *50*, 892–896. [CrossRef]
39. Tahara, N.; Kai, H.; Ishibashi, M.; Nakaura, H.; Kaida, H.; Baba, K.; Hayabuchi, N.; Imaizumi, T. Simvastatin attenuates plaque inflammation: Evaluation by fluorodeoxyglucose positron emission tomography. *J. Am. Coll. Cardiol.* **2006**, *48*, 1825–1831. [CrossRef]
40. Tawakol, A.; Fayad, Z.A.; Mogg, R.; Alon, A.; Klimas, M.T.; Dansky, H.; Subramanian, S.S.; Abdelbaky, A.; Rudd, J.H.; Farkouh, M.E.; et al. Intensification of Statin Therapy Results in a Rapid Reduction in Atherosclerotic Inflammation: Results of A Multi-Center FDG-PET/CT Feasibility Study. *J. Am. Coll. Cardiol.* **2013**, *62*, 909–917. [CrossRef]
41. Botson, J.K.; Peterson, J. Pretreatment and Coadministration With Methotrexate Improved Durability of Pegloticase Response: An Observational, Proof-of-Concept Case Series. *J. Clin. Rheumatol.* **2022**, *28*, e129–e134. [CrossRef] [PubMed] [PubMed Central]
42. Botson, J.K.; Tesser, J.R.P.; Bennett, R.; Kenney, H.M.; Peloso, P.M.; Obermeyer, K.; LaMoreaux, B.; Weinblatt, M.E.; Peterson, J. Pegloticase in Combination With Methotrexate in Patients With Uncontrolled Gout: A Multicenter, Open-label Study (MIRROR). *J. Rheumatol.* **2021**, *48*, 767–774. [CrossRef] [PubMed]
43. Keenan, R.T.; Botson, J.K.; Masri, K.R.; Padnick-Silver, L.; LaMoreaux, B.; Albert, J.A.; Pillinger, M.H. The effect of immunomodulators on the efficacy and tolerability of pegloticase: A systematic review. *Semin. Arthritis Rheum.* **2021**, *51*, 347–352. [CrossRef] [PubMed]
44. Krsytexxa Injection Label. Available online: https://www.accessdata.fda.gov/drugsatfda_docs/label/2012/125293s034lbl.pdf (accessed on 1 April 2012).
45. Fayad, Z.A.; Mani, V.; Woodward, M.; Kallend, D.; Bansilal, S.; Pozza, J.; Burgess, T.; Fuster, V.; Rudd, J.H.; Tawakol, A.; et al. Rationale and design of dal-PLAQUE: A study assessing efficacy and safety of dalcetrapib on progression or regression of atherosclerosis using magnetic resonance imaging and 18F-fluorodeoxyglucose positron emission tomography/computed tomography. *Am. Heart J.* **2011**, *162*, 214–221.e2. [CrossRef] [PubMed] [PubMed Central]
46. Barazani, S.H.; Chi, W.-W.; Pyzik, R.; Chang, H.; Jacobi, A.; O'donnell, T.; Fayad, Z.A.; Ali, Y.; Mani, V. Quantification of uric acid in vasculature of patients with gout using dual-energy computed tomography. *World J. Radiol.* **2020**, *12*, 184–194. [CrossRef] [PubMed] [PubMed Central]
47. Pascual, E.; Addadi, L.; Andrés, M.; Sivera, F. Mechanisms of crystal formation in gout-a structural approach. *Nat. Rev. Rheumatol.* **2015**, *11*, 725–730. [CrossRef]
48. Held, J.; Schwabl, C.; Haschka, D.; Maier, S.; Feuchtner, G.; Widmann, G.; Duftner, C.; Weiss, G.; Klauser, A. Major cardiovascular events in patients with cardiovascular monosodium urate deposits in atherosclerotic plaques. *Rheumatology* **2024**, keae240. [CrossRef] [PubMed]
49. Held, J.; Haschka, D.; Lacaita, P.G.; Feuchtner, G.M.; Klotz, W.; Stofferin, H.; Duftner, C.; Weiss, G.; Klauser, A.S. Review: The Role of Dual-Energy Computed Tomography in Detecting Monosodium Urate Deposits in Vascular Tissues. *Curr. Rheumatol. Rep.* **2024**, *26*, 302–310. [CrossRef] [PubMed] [PubMed Central]
50. Ren, H.; Qu, H.; Zhang, Y.; Gu, Y.; Zhao, Y.; Xu, W.; Wang, W. Detection of monosodium urate depositions and atherosclerotic plaques in the cardiovascular system by dual-energy computed tomography. *Heliyon* **2024**, *10*, e24548. [CrossRef]
51. Yokose, C.; Eide, S.E.; Huber, F.A.; Simeone, F.J.; Ghoshhajra, B.B.; Shojania, K.; Nicolaou, S.; Becce, F.; Choi, H.K. Frequently Encountered artifacts in the application of dual-energy CT to cardiovascular imaging for urate crystals in gout: A matched-control study. *Arthritis Care Res.* **2024**, *76*, 953–963. [CrossRef]
52. Pascart, T.; Carpentier, P.; Choi, H.K.; Norberciak, L.; Ducoulombier, V.; Luraschi, H.; Houvenagel, E.; Legrand, J.; Verclytte, S.; Becce, F.; et al. Identification and characterization of peripheral vascular color-coded DECT lesions in gout and non-gout patients: The VASCURATE study. *Semin. Arthritis Rheum.* **2021**, *51*, 895–902. [CrossRef] [PubMed]
53. Klauser, A.S.; Strobl, S.; Schwabl, C.; Klotz, W.; Feuchtner, G.; Moriggl, B.; Held, J.; Taljanovic, M.; Weaver, J.S.; Reijnierse, M.; et al. Prevalence of Monosodium Urate (MSU) Deposits in Cadavers Detected by Dual-Energy Computed Tomography (DECT). *Diagnostics* **2022**, *12*, 1240. [CrossRef] [PubMed] [PubMed Central]
54. Døssing, A.; Müller, F.C.; Becce, F.; Stamp, L.; Bliddal, H.; Boesen, M. Dual-Energy Computed Tomography for Detection and Characterization of Monosodium Urate, Calcium Pyrophosphate, and Hydroxyapatite: A Phantom Study on Diagnostic Performance. *Invest. Radiol.* **2021**, *56*, 417–424. [CrossRef] [PubMed]

55. Toprover, M.; Mechlin, M.; Fields, T.; Oh, C.; Becce, F.; Pillinger, M.H. Monosodium urate deposition in the lumbosacral spine of patients with gout compared with non-gout controls: A dual-energy CT study. *Semin. Arthritis Rheum.* **2022**, *56*, 152064. [CrossRef]
56. Krystexxa:(Pegloticase). Horizon Therapeutic: Dublin, Ireland; Lake Forest, IL, USA. 2022. Available online: https://www.accessdata.fda.gov/drugsatfda_docs/label/2022/125293s104lbl.pdf (accessed on 1 April 2012).
57. Solomon, D.H.; Giles, J.T.; Liao, K.P.; Ridker, P.M.; Rist, P.M.; Glynn, R.J.; Broderick, R.; Lu, F.; Murray, M.T.; Vanni, K.; et al. Reducing cardiovascular risk with immunomodulators: A randomised active comparator trial among patients with rheumatoid arthritis. *Ann. Rheum. Dis.* **2023**, *82*, 324–330. [CrossRef]
58. Andrés, M.; Quintanilla, M.; Sivera, F.; Sánchez-Payá, J.; Pascual, E.; Vela, P.; Ruiz-Nodar, J. Silent Monosodium Urate Crystal Deposits Are Associated With Severe Coronary Calcification in Asymptomatic Hyperuricemia: An Exploratory Study. *Arthritis Rheumatol.* **2016**, *68*, 1531–1539. [CrossRef] [PubMed]

Disclaimer/Publisher's Note: The statements, opinions and data contained in all publications are solely those of the individual author(s) and contributor(s) and not of MDPI and/or the editor(s). MDPI and/or the editor(s) disclaim responsibility for any injury to people or property resulting from any ideas, methods, instructions or products referred to in the content.